Exploitation of κ-carrageenan aerogels as template for edible oleogel preparation.

Manuscript Details

Manuscript number	FOODHYD_2017_271
Title	Exploitation of κ-carrageenan aerogels as template for edible oleogel preparation
Article type	Research paper

Abstract

In the current research, oleogels were prepared by using k-carrageenan aerogels as template. In particular, hydrogels containing increasing concentration (0.4, 1.0, and 2.0% w/w) of k-carrageenan were firstly converted into alcoholgel and subsequently dried by using supercritical CO2 to obtain aerogels. The latter were porous and structurally stable materials with high mechanical strength. The polymer content affected the aerogel structure: increasing the initial k-carrageenan concentration a coarser structure with larger polymer aggregates was obtained. However, the aerogel obtained at intermediate polymer concentration resulted the firmest one, probably due to the formation of a less aerated and more isotropic structure. Aerogels demonstrated a reduced capacity of water vapor sorption, remaining glassy and porous at room temperature at relative humidity lower that 60%. Aerogels showed a good capacity of oil absorption. The maximum oil loading capacity (about 80 %) was obtained for aerogel containing the highest k-carrageenan content. Thus, it can be concluded that aerogels based on the structuring of water soluble polymers have potential as material for oil absorption and delivery.

Keywords	oleogel; hydrogel; κ-carrageenan; structure; supercritical CO2 drying; sorption kinetics
Taxonomy	Carrageenans, Aerogels

Corresponding Author	Sonia Calligaris
Order of Authors	Lara Manzocco, Fabio Valoppi, Sonia Calligaris, Francesco Andreatta, Sara Spilimbergo, Maria Cristina Nicoli

Suggested reviewers	Giovanna Ferrentino, Edmund Daniel Co, Francesco Donsì, Emin Yilmaz

Submission Files Included in this PDF

File Name [File Type]

cover aerogel.doc [Cover Letter]

Answer to reviewers.docx [Response to Reviewers]

Graphical abstract.tif [Graphical Abstract]

Aerogel_R1.docx [Manuscript File]

Figure 1.tif [Figure]

Figure 2.docx [Figure]

Figure 3.tif [Figure]

Figure 4.tif [Figure]

Supplementary material.docx [Figure]

Highlights.docx [Highlights]

To view all the submission files, including those not included in the PDF, click on the manuscript title on your EVISE Homepage, then click 'Download zip file'.

Dear Editor,

I would like to submit to your attention the manuscript entitled “Exploitation of κ-carrageenan aerogels as template for edible oleogel preparation” (Lara Manzocco, Fabio Valoppi, Sonia Calligaris, Francesco Andreatta, Sara Spilimbergo, Maria Cristina Nicoli for consideration for publication on Food Hydrocolloids.

Oleogels result from liquid oil entrapment in a three-dimensional network without modifying the chemical characteristics of the oil. Although oleogelation is a recent research topic, the possibility to structure oil into self-standing structured solids has received considerable attention in the last decade due to their high potential number of applications of food area.

In the current research, oleogels were prepared by using k-carrageenan aerogels as template. In particular, hydrogels containing increasing concentration of k-carrageenan were firstly converted into alcoholgel and subsequently dried by using supercritical CO_2 to obtain aerogels. The latter were porous and structurally stable materials with high mechanical strength. Aerogels showed a good capacity of oil absorption. The maximum oil loading capacity (about 80 %) was obtained for aerogel containing the highest k-carrageenan content. Thus, it can be concluded that aerogels based on the structuring of water soluble polymers have potential as material for oil absorption and delivery.

We would greatly appreciate your comments on the paper.

Best regards

Sonia Calligaris

Dear Editor,
Please find the revised version of our manuscript (FOODHYD_2017_271). We have endeavoured to take into account or to respond to the Reviewer's comments as indicated below.

We hope that this response is satisfactory and that the manuscript will be suitable for publication in Food Hydrocolloids.

Best regards,
Sonia Calligaris

Reviewer 1

This work is interesting and worthy of publication but the absence of key references makes this reviewer concerned about the work. Firstly, the foam-templating approach was first reported by Patel et al. in 2013, are referenced by the authors. The approach was established there and shown to work. The authors extend the approach to Xanthan gum here. However, for some reason, the authors fail to quote key recent references on foam-templated cellulosic xerogels used to bind oil and stabilize peanut butter and cookie creams, both published in Food Hydrocolloids in 2016. Copies are enclosed with this review.

We thank the reviewer for his/her appreciation of the topic. We also agree with the reviewer that the reference from Tanti et al. (2016) should have been properly quoted. For this reason we added it in the text (lines 59-61). It is our feeling that the proposed approach is different from that reported in the literature since we considered oil absorption by aerogels and not by xerogels, as performed by Patel et al. 2013 and the two papers of Tanti et al., 2016. Please note that Xanthan gum was not used in our experiments, which were developed by using k-carrageenan.

Moreover, the authors also discuss oil binding as a two-step process, without quoting another key reference which has previously used this approach to model oil binding in oleogel systems (Blake et al, 2014).

Blake et al. (2014) was actually cited in the R&D session (line 404). As suggested by the reviewer, mention to this paper was also added in the M&M section (line 267).

Reviewer 2

I congratulate for this very new approach of oleogel preparation. Although it seems hard to apply for actual productions, it is quite novel an approach. Furthermore, the study was well planned and carried out. It is worth to be published.

We thank the reviewer for his/her comments. As the reviewer pointed out, more work needs to be done to apply this approach for an actual production. Mention to this need was reported in the conclusion section of the manuscript (lines 449-451).

Reviewer 3

The paper contains a sufficient work in term of analysis of the k-carrageenan aerogels and the subsequent conversion into oleogels. The authors applied supercritical carbon dioxide drying to obtain the aerogels. They converted the hydrogels with increasing concentration (0.4, 1.0, and 2.0% w/w) of k-carrageenan into alcoholgel and afterwards they dried them.

In the introduction the authors stated that supercritical carbon dioxide drying shown several advantages in terms of product quality compared to air and freeze drying. These assumptions could be accepted considering that several studies have been published so far claiming the potential of supercritical carbon dioxide drying. However, it is completely unacceptable the lack of the experimental design presented in this study. The authors just applied one pressure and one temperature (11 MPa and 45 °C) to obtain aerogels at different concentrations of k-carrageenan. How did they choose this conditions? As the process is so innovative, I suggest to test several conditions of pressure and temperature to investigate the effect of the process on the microstructure and oil absorption of the product.
In materials and methods, the authors wrote that the drying was performed "….at 3.5 NL/min using a micrometric valve. After 3 h of drying, the outlet flow rate was increased to 5.0 NL/min for additional 4 h, maintaining the same pressure. Finally, flow rate was increased to 6.0 NL/min for 1 h." Why did they use this drying procedure? Did they find references supporting it? Probably no differences (or significant differences) could be observed drying at 3.5 NL/min or 6.0 NL/min or combining several carbon dioxide flow rates. But the authors needed to prove it.

We thank the reviewer for his/her suggestions and comments. The conditions adopted in the experiments were selected based on different considerations:

Pressure and temperature above the critical point of carbon dioxide were selected based on pilot plant performance. Flow rate program was selected on the basis of preliminary trials. The latter were performed in a wide range of flow rate from 2.0 to 8.0 NL/min. The adopted program was selected since associated with short drying time while guarantee the structural integrity of the sample. Excessive flow rates in the initial part of the drying process actually produced large cracks on the sample surface and were discarded. By contrast, initial flow rate was kept low and progressively increased up to the final steps of drying. This information was added in the manuscript (lines 140-143 and lines 151-156)

In materials and methods, Table 1 could be erased and included in the text (paragraph 2.2 hydrogel preparation).

We agree with the reviewer and text was modified accordingly (lines 123-125).

In results and discussion, it was stated that "The removal of ethanol resulted complete after 6, 7, and 8 h of drying for samples containing 0.4, 1.0 and 2.0 % (w/w) k-C."
How did the authors assume that drying was complete after 6, 7, and 8 h? What did they measure? I suggest to include the drying kinetics to show the efficiency of the process at different conditions of pressure and temperature. An optimization of the process parameters will highly increase the scientific value of the manuscript.

The drying kinetics were assessed recording the evolution of ethanol concentration over time using a digital alcoholmeter (see Material and Method section, lines 160-161). Drying kinetics were added as supplementary information (Figure S1).

Hydrogel

Solvent substitution + Supercritical CO_2 drying

Aerogel

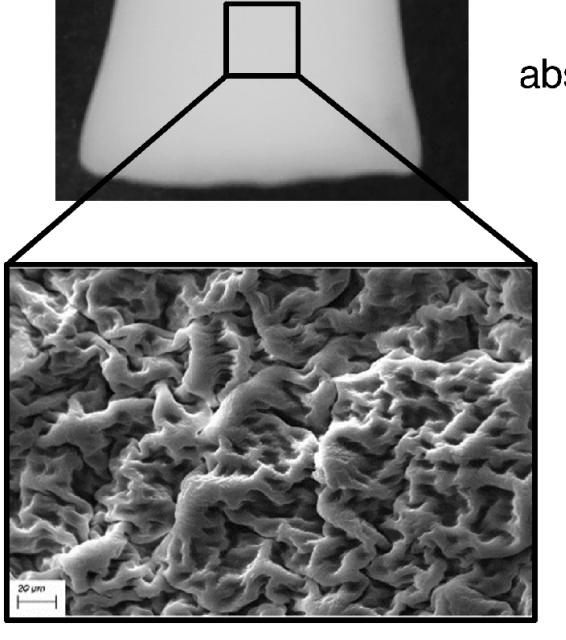

Oil absorption

Oleogel

Oil loading capacity up to 80% (w/w)

Exploitation of κ-carrageenan aerogels as template for edible oleogel preparation

Lara Manzocco[a], Fabio Valoppi[a,1], Sonia Calligaris[a,*], Francesco Andreatta[b], Sara Spilimbergo[c], Maria Cristina Nicoli[a]

Affiliation

[a] Dipartimento di Scienze AgroAlimentari, Ambientali e Animali, Università di Udine, Via Sondrio 2/A, Udine, Italy

[b] Dipartimento Politecnico di Ingegneria e Architettura, Università di Udine, Via delle Scienze 206, Udine, Italy

[c] Dipartimento di Ingegneria Industriale, Università di Padova, Via Marzolo 9, Padova, Italy

e-mail addresses:

Lara Manzocco: lara.manzocco@uniud.it

Fabio Valoppi: fabio.valoppi@unibz.it

Sonia Calligaris: sonia.calligaris@uniud.it

Francesco Andreatta: francesco.andreatta@uniud.it

Sara Spilimbergo: sara.spilimbergo@unipd.it

Maria Cristina Nicoli: mariacristina.nicoli@uniud.it

[*]Corresponding author

Phone +39 0432 558571 ; fax: +39 0432 558100; e-mail: sonia.caligaris@uniud.it

Present address

[1] Facoltà di Scienze e Tecnologie, Libera Università di Bolzano-Bozen, Piazza Università 1, Bolzano, Italy

Abstract

In the current research, oleogels were prepared by using k-carrageenan aerogels as template. In particular, hydrogels containing increasing concentration (0.4, 1.0, and 2.0% w/w) of k-carrageenan were firstly converted into alcoholgel and subsequently dried by using supercritical CO_2 to obtain aerogels. The latter were porous and structurally stable materials with high mechanical strength. The polymer content affected the aerogel structure: increasing the initial k-carrageenan concentration a coarser structure with larger polymer aggregates was obtained. However, the aerogel obtained at intermediate polymer concentration resulted the firmest one, probably due to the formation of a less aerated and more isotropic structure. Aerogels demonstrated a reduced capacity of water vapor sorption, remaining glassy and porous at room temperature at relative humidity lower that 60%. Aerogels showed a good capacity of oil absorption. The maximum oil loading capacity (about 80 %) was obtained for aerogel containing the highest k-carrageenan content. Thus, it can be concluded that aerogels based on the structuring of water soluble polymers have potential as material for oil absorption and delivery.

Keywords: oleogel; hydrogel; κ-carrageenan; structure; supercritical CO_2 drying; sorption kinetics

1. Introduction

Oleogels result from liquid oil entrapment in a three-dimensional network without modifying the chemical characteristics of the oil. Although oleogelation is a recent research topic, the possibility to structure oil into self-standing structured solids has received considerable attention in the last decade since they have been proposed as hydrogenated/saturated fat replacers, oil migration inhibitors, oil binders, and oxidation protective systems (Da Pieve, Calligaris, Panozzo, Arrighetti, & Nicoli, 2011; Patel et al., 2014; Stortz & Marangoni, 2013; Yilmaz & Ogutcu, 2015; Zetzl, Marangoni, & Barbut, 2012; Zulim Botega, Marangoni, Smith, & Goff, 2013).

The simplest approach to oil gelation is based on the formation of crystalline networks by self-assemble lipid additives (Co & Marangoni, 2012) or by networking of chemically modified biopolymers such as ethyl cellulose and hydrolyzed chitin (Co & Marangoni, 2012; Laredo, Barbut, & Marangoni, 2011; Nikiforidis & Scholten, 2015). However, oleogels could also be generated by absorption of liquid oil into a porous template made of a dried polymeric network of gelatin, xanthan gum, methylcellulose and hydroxypropyl methylcellulose (Patel & Dewettinck, 2016; Patel, Schatteman, Lesaffer, & Dewettinck, 2013; Tanti, Barbut, & Marangoni, 2016a, 2016b). To this aim, the polymer is pre-hydrated to form a hydrogel. The latter is then dried to block the polymer network and obtain a porous material that can uptake oil. However, this procedure is hardly applied due to structural collapse during hydrogel drying. Traditional air drying is actually unable to prevent hydrogel collapse due to the formation of liquid-vapor menisci in the gel pores. This produces a capillary pressure gradient that causes pore collapse, leading to xerogel materials with limited oil sorption capacity (Scherer & Smith, 1995). Similarly, freeze-drying of hydrogels causes intense network stress due to formation of crystals before drying. As a result, cryogels undergo internal breakage of polymer network and surface cracking (Garcia-Gonzalez, Camino-Rey, Alnaief, Zetzl, & Smirnova, 2012). To prevent pore collapse phenomena and maintain as much as possible the hydrogel network

architecture, a two-step procedure may be exploited: firstly, solvent exchange is carried out so that water in the hydrogel is replaced by ethanol to obtain an alcoholgel; secondly, ethanol is extracted from the alcoholgel by supercritical carbon dioxide drying to obtain an aerogel (Garcia-Gonzalez et al., 2012). Supercritical drying prevents structure collapse since it does not involve vapor transitions nor intense surface tensions in the pores. The resulting aerogels are thus low density and highly porous materials (Gesser & Goswami, 1989; Hrubesh & Poco, 1995).

Most aerogels are inorganic, being often made of silica, metal oxides or polystyrenes (Du, Zhou, Zhang, & Shen, 2013; Gesser & Goswami, 1989; Pierre & Pajonk, 2002). They are lightweight materials with high mechanic strength and excellent thermal insulation and dielectric properties (Pierre & Pajonk, 2002). However, according to Pierre & Pajonk (2002), not only inorganic polymerizing agents but all organic biopolymers are potential candidates to form aerogels. To this regard, the preparation of aerogels from different polysaccharides, including starch, cellulose, pectin, and carrageenan, have been recently reviewed by Mikkonen, Parikka, Ghafar, & Tenkanen (2013) and Ivanovic, Milovanovic, & Zizovic (2016). These materials have been proposed for packaging purposes but also for encapsulation and controlled release of drugs, aroma or antioxidants. They have also been shown to quickly absorb aqueous solutions and surfactants by capillary forces, due to the open pore structure and large surface area (Escudero, Robitzer, Di Renzo, & Quignard, 2009; Mallepally, Bernard, Marin, Ward, & McHugh, 2013). Recently, aerogels have been proposed also as oil carrier. Comin, Temelli, & Saldana (2012) studied the oil impregnation capacity of β-glucan aerogels. In this case, the highest impregnation capacity was about 65%. Similarly, Ahmadi, Madadlou, & Saboury (2016) proposed aerogels made of whey proteins and crystalline cellulose. The latter presented a maximum oil loading capacity of about 70%.

95 Based on this information, the possibility to obtain food-grade aerogels with high oil loading
96 capacity could open new opportunities in the exploitation of aerogels for novel food
97 applications.
98 This work represents a first attempt to develop food-grade oleogels by oil sorption into aerogels
99 by using κ-carrageenan as structuring biopolymer. This widely used food additive was chosen
100 because, in the presence of K^+, it forms hydrogels with a tubular architecture, which could be
101 particularly interesting for oil sorption (Dunstan et al., 2001). κ-carrageenan hydrogels with
102 different concentration were converted to alcoholgels by a solvent exchange procedure. Ethanol
103 was then removed from the alcoholgel by supercritical carbon dioxide drying to obtain the
104 aerogels. The supercritical drying has been indicated as the most promising drying methodology
105 to obtain aerogels mainly because it prevents the gel structure from pore physical collapse
106 phenomenon and shrinkage upon solvent removal (Ivanovic et al., 2016). κ -carrageenan based
107 aerogel were characterized for appearance, network density, firmness, microstructure, water
108 vapor adsorption and glass transition. Finally, the capability of aerogels to absorb sunflower oil
109 and form oleogels was evaluated.
110

111 **2. Materials and methods**

112 **2.1 Materials**

113 κ-carrageenan (κ-C) was purchased from Sigma-Aldrich (Milan, Italy); lithium chloride (LiCl),
114 calcium chloride hexahydrate ($CaCl_2 \cdot 6H_2O$), potassium carbonate (K_2CO_3), sodium chloride
115 (NaCl), potassium acetate (CH_3COOK), potassium chloride (KCl), and potassium sulfate
116 (K_2SO_4) were purchased from Carlo Erba Reagents (Milan, Italy); absolute ethanol was
117 purchased from J.T. Baker (Griesheim, Germany); phosphorus pentoxide (P_2O_5) was purchased
118 from Chem-Lab NV (Zedelgem, Belgium); sunflower oil was purchased in a local market. All
119 solutions were prepared using milli-Q water.
120

2.2 Hydrogel preparation

Aqueous suspensions containing 0.4, 1.0, or 2.0% (w/w) κ-C and 1.0, 1.0 or 2.0 % (w/w) KCl, respectively, were prepared. In particular, κ-C was slowly added to the KCl aqueous solution at 90 °C under stirring. The homogeneous κ-C suspension was then poured into cylindrical molds of 2.9 cm diameter and 12 cm height. Samples were cooled in an ice bath and stored for 1 day at 4 °C before analysis or further processing.

2.3 Hydrogel to alcoholgel conversion by solvent substitution

κ-C hydrogels were cut in cylinders with a height of about 4.5 cm and diameter of 2.9 cm and were maintained for 1 day into aqueous solutions of ethanol with increasing concentrations (25, 50, 75% v/v). Finally, samples were introduced into absolute ethanol twice (the first time for 8 h and the second one for 1 day) in order to remove residual water. The ratio between hydrogel and ethanol solutions was 1:8 (v/v). Conversion was carried out at room temperature (about 22 °C).

2.4 Alcoholgel to aerogel conversion by supercritical CO_2 drying

Alcoholgels were converted to aerogel by supercritical CO_2 drying using the apparatus (Figure 1) developed at the Department of Agricultural, Food, Environmental and Animal Sciences of the University of Udine. Preliminary tests were carried out to define supercritical CO_2 drying conditions to obtain aerogels in the available equipment. Based on these preliminary results, aerogels were produced after their maintenance in a continuous flow of supercritical CO_2 at 11 ± 1 MPa and 45 °C. Liquid carbon dioxide (purity 99.995%, Sapio, Monza, Italy) was cooled to 4 °C using a F34-ED chiller (C; Julabo, Milano, Itlay) after been filtered with a 15 μm filter (B_1; Ham-Let, Milano, Italy). Subsequently, CO_2 was pressurized at 11 ± 1 MPa with an Orlita MhS35/10 diaphragm pump (D; ProMinent Italiana S.r.l., Bolzano, Italy) and heated to 45 °C using a water bath connected to a CB8 − 30e thermostatic bath (G; Heto, Allerød, Denmark).

147 Before pressurization, alcoholgel sample was placed inside the stainless steel cylindrical reactor
148 (E, volume ~265 mL) with two screwed caps, each one equipped with a sintered stainless steel
149 filter that allowed a uniform distribution of the CO_2 during drying. Different combinations of
150 supercritical CO_2 flows in the range from 2.0 to 8.0 NL/min were initially tested. The
151 combination allowing drying time to be minimized while maintaining the structural integrity of
152 the material were selected by visual assessment of the absence of surface cracks on the samples.
153 The adopted conditions were: the outlet flow through the reactor was 3.5 NL/min for 3 h; 5.0
154 NL/min for subsequent 4 h and 6.0 NL/min for subsequent 1 h. Finally, a slow decompression
155 from 11 MPa to atmospheric pressure was carried out at 6.0 NL/min in 30 min. The outlet flow
156 was set by a micrometric valve (V_4) and controlled with a RAGK41 rotameter (H; Rota
157 Yokogawa, Milan, Italy). To avoid malfunctioning of the rotameter, CO_2 was filtered with a 40
158 μm filter (B_2; Ham-Let, Milano, Italy). Ethanol content in the gaseous outlet was measured
159 using a AL9000L digital alcoholmeter (L; Alcoscan, Milan, Italy) every 60 min. In order to
160 carefully control temperature and pressure during experiments, a thermocouple (TT) connected
161 to a digital data logger (F) and a manometer (PT2) were used. The valves V_3 and V_4 were heated
162 in a water bath connected to a thermostatic bath (G) to prevent freezing during decompression.
163 In order to assure an adequate heat exchange in the water bath, a small water pump (P) was
164 used.
165 Aerogels were stored in a desiccator containing P_2O_5 at room temperature until use.
166
167 **2.5 Aerogel to oleogel conversion by oil absorption**
168 Aerogel samples were introduced into 250 mL beakers previously filled with 125 mL of
169 sunflower oil. At defined time intervals during conversion from aerogel to oleogel, samples
170 were withdrawn, wiped with absorbing paper and weighted. Absorbed oil was expressed as the
171 ratio between weight gain at time *t* and the initial weight of the aerogel sample. The immersion

of aerogel into oil was prolonged until a constant weight after two consequent readings was reached.

2.6 Analytical determinations

2.6.1 Volume and network density

Sample volume was calculated as the volume of the cylinder whose diameter and height were measured by a CD-15APXR digital caliper (Absolute AOS Digimatic, Mitutoyo Corporation, Kanagawa, Japan). Volume changes following conversion of hydrogel to alcoholgel and aerogel were expressed as the percentage ratio between the variation of sample volume and volume of the corresponding hydrogel. Network density was then calculated as the ratio between aerogel sample weight and volume of hydro-, alcohol-, aero- or oleogel samples.

2.6.2 Firmness

Firmness was measured by uniaxial compression test using an Instron 4301 (Instron LTD., High Wycombe, UK). The instrumental settings and operations were accomplished using the software Automated Materials Testing System (version 5, Series IX, Instron LTD., High Wycombe, UK). In particular, hydrogel and alcoholgel samples (about 2.9 cm diameter and 1.5 cm height) were tested using a 6.2 mm diameter cylindrical probe mounted on a 100 N compression head at a 25 mm/min crosshead speed. Force–distance curves were obtained from the compression tests and firmness was taken as the maximum force (N) required to penetrated the sample for 5 mm. Aerogel and oleogel samples (about 1 cm diameter and 3 mm height) were tested using a 12.7 mm diameter cylindrical probe mounted on a 1000 N compression head at a 25 mm/min crosshead speed. Force–distance curves were obtained from the compression tests and firmness was taken as the maximum force (N) required to compress the sample by 1 mm. The analyses were repeated at least 3 times for each sample.

198

199 ***2.6.3 Image acquisition***

200 Sample images were acquired using an image acquisition cabinet (Immagini & Computer,
201 Bareggio, Italy) equipped with a digital camera (EOS 550D, Canon, Milano, Italy). In
202 particular, the digital camera was placed on an adjustable stand positioned 45 cm above a black
203 or white cardboard base where the samples were placed. Light was provided by 4 100 W frosted
204 photographic floodlights, in a position allowing minimum shadow and glare. Images were
205 saved in *jpeg* format resulting in 3456×2304 pixels.

206

207 ***2.6.4 Scanning Electron Microscopy (SEM)***

208 Aerogel samples were mounted on aluminum sample holders and sputter coated with 10 nm of
209 gold using a Sputter Coater 108 auto (Cressington Scientific Instruments, Watford, United
210 Kingdom). The aluminum holder was transferred to the SEM unit (EVO 40XVP, Carl Zeiss,
211 Milan, Italy), which was at ambient temperature and under vacuum. Samples were imaged using
212 an acceleration voltage of 20 kV and SmartSEM v. 5.09 (Carl Zeiss, Milan, Italy) application
213 software was used to capture images of the samples. Images were saved in *tiff* format resulting
214 in 1696×2048 pixels.

215

216 ***2.6.5 Water vapor sorption***

217 Aerogel samples were weighted and transferred into a dried weighting bottle. The latter was
218 then transferred into desiccators containing LiCl, CH_3COOK, $CaCl_2$, K_2CO_3, NaCl, KCl, and
219 K_2SO_4 saturated solutions with equilibrium relative humidity (ERH%) values of 11, 25, 31, 43,
220 75, 86, and 96%, respectively. Samples were kept inside desiccators until constant weight was
221 reached. The Brunauer-Emmet-Teller (BET) sorption isotherm model (eq. 1) was fitted into
222 water sorption data (Brunauer, Emmett, & Teller, 1938).

223 $$\frac{a_w}{m \cdot (1 - a_w)} = \frac{1}{m_0 \cdot c} + \frac{c - 1}{m_0 \cdot c} \cdot a_w \quad (1)$$

where a_w is the water activity, m is the moisture of the sample expressed as ratio between the weight (g) of absorbed water and the weight (g) of dry matter, m_0 is the moisture of the water monolayer, and c is an experimental constant.

2.6.6 Differential Scanning Calorimetry (DSC)

DSC analysis was carried out using a TA4000 differential scanning calorimeter (Mettler-Toledo, Greifensee, Swiss) connected to a GraphWare software TAT72.2/5 (Mettler-Toledo). Heat flow calibration was achieved using indium (heat of fusion 28.45 J/g). Temperature calibration was carried out using hexane (m.p. -93.5 °C), water (m.p. 0.0 °C) and indium (m.p. 156.6 °C). Samples were prepared by carefully weighing around 10 mg of hydrogel or aerogel in 160 mL aluminum DSC pans, closed with hermetic sealing. An empty pan was used as a reference in the DSC cell.

Aerogel samples equilibrated at different a_w values were heated from -150 to 250 °C. The scan speed was set at 10 °C/min and samples were analyzed under nitrogen flow (20 mL/min). The start of melting transition was taken as on-set (T_{on}) point of transition, that is the point at which the extrapolated baseline intersects the extrapolated tangent of the calorimetric peak in the transition state. Total peak enthalpy (ΔH_m) was obtained by integration of the melting curve. T_g was determined from the on-set temperature of the glass transition of aerogels. The machine equipment program STARe ver. 8.10 (Mettler-Toledo, Greifensee, Switzerland) was used to plot and analyze the thermal data.

The amount of frozen water was then calculated as the ratio between aerogel ΔH_m and pure ice ΔH_m (333.5 J/g). The concentration of the maximally cryo-concentrated solution (c'_g) was calculated from the amount of unfrozen water and total solids.

2.6.7 State diagram and modified state diagram

Aerogel state diagrams were obtained plotting the T_g values for samples equilibrated at different ERH% as a function of mass fraction of the sample. The obtained curve was fitted using the Gordon-Taylor equation (eq. 2) (Gordon & Taylor, 1952).

$$T_g = \frac{w_1 T_{g1} + k w_2 T_{g2}}{w_1 + k w_2} \quad (2)$$

where T_{g1} is the glass transition temperature of the amorphous solute, T_{g2} is the glass transition temperature of the solvent (-137.5°C), w_1 and w_2 are the mass fraction of the solute and the solvent, respectively, and k is an experimental constant.

The modified state diagram was then obtained plotting the T_g values for samples equilibrated at different ERH% as a function of their a_w values.

2.6.8 Oil absorption kinetics

Oil content of the oleogel was defined as the percentage ratio between the maximum amount of absorbed oil and the weight of the oleogel.

Oil absorption capacity was calculated as the ratio between weight gain at time t and aerogel network density. The kinetics of oil absorption were then elaborated by fitting a two-phase exponential decay model (eq. 3) to absorption data (Blake, Co, & Marangoni, 2014).

$$y = y_{fast}\left(1 - e^{\left(-k_{fast}t\right)}\right) + y_{slow}\left(1 - e^{\left(-k_{slow}t\right)}\right) \quad (3)$$

$$y_{max} = y_{fast} + y_{slow} \quad (4)$$

where y_{fast} and y_{slow} are the asymptote values of the fast- and slow-decaying components, respectively, k_{fast} and k_{slow} are the rate constants for the fast- and slow-decaying component, respectively, and y_{max} is the maximum amount of absorbed oil when time t tends to infinite and is the sum of y_{fast} and y_{slow} (eq. 4). y_{max} can also be considered the theoretical plateau value.

2.6.9 Oil holding capacity (OHC)

Around 100 - 200 mg of oleogel was placed into 1.5 mL microtubes between two pieces of absorbing paper. Samples were centrifuged at 13,000 rpm (15,871 x *g*) for 30 min using a microcentrifuge (Mikro 120, Hettich Zentrifugen, Andreas Hettich GmbH and Co, Tuttlingen, Germany). Oil holding capacity (OHC) was computed as the percentage ratio among the weight of oil retained in the oleogel after centrifugation and total weight of oil in the sample.

2.6.10 Data analysis

All determinations were expressed as the mean ± standard error (SE) of at least two measurements from two experiment replicates ($n \geq 4$), if not otherwise specified. Statistical analysis was performed by using R v. 3.0.2 (The R foundation for Statistical Computing). Bartlett's test was used to check the homogeneity of variance, one way ANOVA was carried out and Tukey-test was used as post-hoc test to determine statistical significant differences among means ($p < 0.05$). Linear regression analysis by least squares minimization was performed using GraphPad Prism v.5.03 (GraphPad Software, San Diego, USA). The goodness of fit was evaluated on the basis of statistical parameters of fitting (R^2, p, standard error) and the residual analysis. Non-linear regression analysis of T_g values as a function of aerogel mass fraction was performed on TableCurve 2D software (Jandel Scientific, ver. 5.01). Levenberg–Marquardt algorithm was used to perform least squares function minimization and the goodness of fit was evaluated on the basis of statistical parameters of fitting (R^2, p, standard error) and the residual analysis.

3. Results and discussion

3.1 From hydrogel to aerogel

κ-carrageenan (κ-C) hydrogels were used as template to obtain aerogels by applying a solvent exchange procedure. Hydrogels were initially formed thanks to the well-known ability of k-C random coils to transit to a double helix conformation. The double helices, in the presence of

301 monovalent ions, such as potassium (K^+), aggregated in water forming a gelled system
302 (Rinaudo, 2008; Rochas & Rinaudo, 1984). Hydrogels containing different concentration of k-
303 C appeared as self-standing materials with a network density and firmness that linearly
304 increased as the concentration of the structuring polymer increased ($R^2 > 0.99$) (Table 1). This
305 was due, as known, to the formation of a higher number of junction zones among the double
306 helices (Rinaudo, 2008). The hydrogels were firstly converted to alcoholgels by substituting
307 the water solvent with ethanol. Ethanol was then removed from the alcoholgel by a continuous
308 flow of supercritical CO_2, obtaining the aerogels. The removal of ethanol resulted complete
309 after 6, 7, and 8 h of drying for samples containing 0.4, 1.0 and 2.0 % (w/w) k-C (see Figure
310 S1 in supplementary material).
311 Figure 2 shows the visual appearance of hydrogels, alcoholgels and aerogels. It is evident that
312 gel characteristics changed upon solvent exchange. Aerogels appeared completely opaque,
313 differently from hydrogel and alcoholgel, suggesting the aerogel can be regarded as a porous
314 material. Porosity would favor intense light scattering, providing a dense and white appearance.
315 Turning hydrogels into alcoholgels and then aerogels also promoted an intense shrinkage
316 (Figure 2). The latter can be probably attributable to the different structural organization of the
317 gel network depending on the solvent nature. During the first solvent substitution, ethanol is
318 forced to diffuse through the k-C network even if this polymer is insoluble in ethanol
319 (Therkelsen, 1993). For this reason, ethanol difficulty interacts with k-C and is unable to fill all
320 the space previously occupied by water. The interactions among k-C chains became thus
321 stronger, leading to gel shrinkage. The alcohol removal caused a further shrinkage, probably
322 indicating a collapse of the structure upon drying (Figure 2). k-C concentration in the hydrogels
323 negatively affected the level of shrinkage, so that volume contraction progressively decreased
324 as k-C concentration increase. This suggests that samples richer in structured polymer chains
325 were less prone to shrinkage and begot a more porous aerogel structure.

As a consequence of shrinkage, the gel network density progressively increased moving from hydrogel to aerogel, at all k-C concentrations (Table 1). This result confirms the hypothesis that solvent substitution led to a reduction of the distance among polymer network chains. It is interesting to note that the network density of aerogels decreased as k-C concentration increased, differently from hydrogels and alcoholgels. This suggests that the higher the polymer content, the more porous the aerogel structure. A maximum firmness value was observed for sample at intermediate k-C concentration. It could be inferred that the higher resistance to mechanical deformation of this sample could be the result of less aerated and/or more isotropic aerogels. To confirm this hypothesis, SEM analysis of aerogels was performed. Images in Figure 2 revealed the presence of a compact matrix of k-C with superficial pores in all samples, even if with some morphological differences. Sample at the lowest k-C concentration was characterized by a compact structure embedding restricted porous areas. The latter showed a fine-grain and appeared evenly distributed in the aerogel with intermediate k-C content. Finally, sample with the highest k-C content showed a coarse structure with larger polymer aggregates as well as cracks and microchannels onto the surface. Results clearly indicate that aerated structures were achieved when hydrogel structural collapse was hindered by increasing its initial polymer concentration.

In order to investigate the properties of the developed aerogels, their capacity of absorbing water vapor was evaluated. Samples were thus equilibrated at constant temperature and different relative humidity to obtain their sorption isotherms. Moisture content data were then modelled as a function of a_w, using the procedure proposed by Brunauer et al. (1938). Regression analysis showed good determination coefficients (> 0.85) and statistically significant model parameters ($p < 0.05$). The monolayer water content (m_0) and the BET constant (c) were thus estimated (Table 2).

The m_0 parameter showed comparable values for the three aerogels. The constant c showed values between 2 and 50 revealing the presence of a type II isotherm (Al-Muhtaseb, McMinn,

& Magee, 2002; Brunauer, Deming, Deming, & Teller, 1940). This means that the aerogels were characterized by a poor capacity of water vapor sorption since an increase in the relative humidity was reflected into a great a_w increase. In other words, water vapor difficulty interacted with the porous aerogel structure. Its swelling and solvation only occurred when direct hydration of the aerogels was carried out by water immersion (data not shown).

To study the physical stability of the aerogels, DSC analysis was performed. Aerogels were characterized by a glass transition temperature of 180 ± 1 °C, indicating that they were in the glassy state at room temperature. The effect of equilibration at different ERH% on aerogel glass transition temperature was then studied. Glass transition temperature data were modeled as a function of mass fraction using the approach proposed by Gordon & Taylor (1952). Non-linear regression analysis showed good determination coefficients (> 0.93) and significant ($p < 0.001$) values of the model experimental constant (k) (Table 2). Also in this case, no differences among samples were detected.

The modified state diagrams of the aerogels were thus obtained combining the water vapor sorption curve with the glass transition temperature one, and resulted comparable for the three aerogels. This suggests that the ERH% dependence of aerogel physical stability is mainly governed by the intrinsic properties of k-C rather than by the structure of the aerogel. As an example, Figure 3 shows the modified state diagram of the aerogel obtained from a hydrogel containing 1% k-C.

At room temperature, the system was below the glass transition temperature up to an a_w value of 0.6. However, when an amount of water equal to the 10% of the aerogel sample mass was absorbed, the system decreases its glass transition temperature below 20 °C and a transition to the rubber state was observed. This transition led to a structural collapse and the system became thermodynamically unstable. Based on these data, the aerogels here developed would remain glassy and porous at room temperature if maintained at ERH lower than 60%. For these reasons,

aerogels can be easily stored for prolonged time if protected from atmospheric moisture through appropriate packaging.

3.2 From aerogels to oleogels

Based on their physical properties, aerogels could be exploited to entrap liquid oil, potentially leading to oleogels. The capacity of aerogels to absorb oil was thus evaluated (Figure 4).

Oil absorption progressively increased during immersion in oil and was considered complete after the plateau value was reached (Figure 4A). The rate of oil absorption was also greatly affected by the aerogel structure, so that the maximum amount of absorbed oil was reached after 3, 24 and 48 h for samples containing 0.4, 1.0 and 2.0% k-C, respectively. Data in Figure 4A were further elaborated to evidence the effect of the network density on oil absorption. Oil absorption capacity of the aerogel was computed as the ratio between absorbed oil and network density. Normalization of absorbed oil based on network density (Figure 4B) clearly shows that the capacity of the aerogel to absorb oil progressively increased in the order 0.4 < 1.0 < 2.0% k-C. This suggests that the aerogels, which had experienced a lower level of structural collapse (lower shrinkage), also showed a higher capacity of oil absorption, regardless the network density. In other words, the capacity of oil to be entrapped in the aerogel depends not only on the density of the polymer network but also on its architecture. Liquid absorption by a porous material is actually affected by several factors such as number, dimension and size distribution of pores, pores tortuosity and internal surface (i.e. roughness) (Bear, 1972; Khosravi & Azizian, 2016). The diameter of the pores is known to steer the rate of oil absorption while the number and length of pores affect the amount of absorbed oil. To further investigate these aspects, kinetics of aerogel oil absorption were analyzed. In particular, data shown in Figure 4B were elaborated by fitting a two-phase exponential decay model (eq. 3) (Blake et al., 2014). This model was chosen since it describes oil absorption kinetics as a result of two different components. The fast component, which is related to pore diameter, and the slow component,

403 which accounts for pore number and length. Non-linear regression analysis showed good
404 determination coefficient (> 0.99) and significant ($p < 0.001$) model parameters (Table 3).
405 The rate constant for the fast-decaying component (k_{fast}) resulted always higher than the slow
406 one, indicating that the limiting factor of the initial phase of oil absorption was pore size. The
407 value of k_{fast} decreased by increasing the aerogel network density. As discussed by Khosravi &
408 Azizian (2016), lower value of k_{fast} could be related to the presence of pores with larger
409 diameter, which are known to be less effective in initial oil uptake. These larger pores were
410 probably more numerous and longer according to the sample order 2.0 > 1.0 > 0.4% (w/w) k-
411 C in the initial hydrogel. This result is in agreement with the microscopic structure of the
412 aerogels (Figure 2) and gives reason for the increasing overall absorption of oil, as indicated by
413 the higher value of y_{max} (Table 3).
414 Samples after absorption of the maximum amount of oil can be regarded as oleogels. Table 4
415 shows their visual appearance, composition, firmness and oil holding capacity.
416 Oleogels obtained from hydrogels containing 0.4 and 1.0% (w/w) k-C were able to entrap
417 around 2.5 times their initial weight, whereas the aerogel obtained from 2.0% k-C hydrogel
418 held *circa* 4.5 times its initial weight (Figure 4A). Firmness of oleogels showed the same trend
419 observed for aerogels (Table 1) with a maximum value for sample containing 1.0% (w/w) k-C.
420 The maximum loading capacity resulted about 81% (w/w) that is higher than that reported for
421 aerogels containing other food-grade biopolymers, such as β-glucans (Comin et al., 2012) and
422 whey proteins (Ahmadi et al., 2016). Finally, the capability of the oleogels in retaining absorbed
423 oil was finally assessed by an accelerated oil release test based on centrifugation. The highest
424 values of oil holding capacity (OHC) were recorded for samples containing 0.4 and 1.0% (w/w)
425 κ-C in the initial hydrogel. By contrast, aerogels from 2.0% (w/w) κ-C hydrogel showed a lower
426 ability to retain oil. In other words, this sample, which was characterized by a higher number
427 of longer pores absorbed the highest amounts of oil (Figure 4) that can be easily released upon
428 centrifugation. This suggest that oil is physically entrapped in the system cavities.

Conclusions

κ-carrageenan aerogels resulted to be highly porous and structurally stable materials with high mechanic strength. Similarly to other organic aerogels, they were made from renewable sources and were completely biodegradable. Given these properties, they could be used for a number of different applications, including thermal and electric insulation but also development of novel packaging materials and selective carriers for drugs, nutrients, aroma compounds or additives. In the present work, a novel application of κ-carrageenan aerogels was studied. The latter were actually demonstrated to uptake large amounts of oil without compromising their structural integrity and leading to stiff oleogels. Oil content and retention depended on the aerogel architectural organization, as described by the pore number, size and length. These results suggest that k-carrageenan based aerogels could be used to absorb lipophilic molecules, including unintentionally discharged oil spills. Reversely, κ-carrageenan oleogels could be exploited in the food, pharmaceutical or cosmetic sectors for pioneering applications. The results acquired were relevant to κ-carrageenan oleogels but the methodology here developed could be definitely extended to other biopolymers. Further research is thus needed to explore this possibility and obtain food grade oleogels with tailored characteristics.

Acknowledgements

LM and SC conceived the study and carried out the experiments in conjunction with FV. FA carried out the SEM analysis. SS supported the development of supercritical CO_2 equipment. All authors participated in manuscript revision and discussion, coordinated and critiqued by LM, SC and MCN. Authors would like to thank Dr. Michele Magna for his technical help.

Fundings

This research did not receive any specific grant from funding agencies in the public, commercial, or not-for-profit sectors.

References

Ahmadi, M., Madadlou, A., & Saboury, A. A. (2016). Whey protein aerogel as blended with cellulose crystalline particles or loaded with fish oil. *Food Chemistry, 196*, 1016-1022.

Al-Muhtaseb, A. H., McMinn, W. A. M., & Magee, T. R. A. (2002). Moisture Sorption Isotherm Characteristics of Food Products: A Review. *Food and Bioproducts Processing, 80*, 118-128.

Bear, J. (1972). *Dynamics of fluids in porous media* (J. Bear Ed.). New York (USA): American Elsevier Publishing Company, inc.

Blake, A. I., Co, E. D., & Marangoni, A. G. (2014). Structure and Physical Properties of Plant Wax Crystal Networks and Their Relationship to Oil Binding Capacity. *Journal of the American Oil Chemists' Society, 91*, 885-903.

Brunauer, S., Deming, L. S., Deming, W. E., & Teller, E. (1940). On a Theory of the van der Waals Adsorption of Gases. *Journal of the American Chemical Society, 62*, 1723-1732.

Brunauer, S., Emmett, P. H., & Teller, E. (1938). Adsorption of Gases in Multimolecular Layers. *Journal of the American Chemical Society, 60*, 309-319.

Co, E. D., & Marangoni, A. G. (2012). Organogels: An Alternative Edible Oil-Structuring Method. *Journal of the American Oil Chemists' Society, 89*, 749-780.

Comin, L. M., Temelli, F., & Saldana, M. D. A. (2012). Barley beta-glucan aerogels as a carrier for flax oil via supercritical CO2. *Journal of Food Engineering, 111*, 625-631.

Da Pieve, S., Calligaris, S., Panozzo, A., Arrighetti, G., & Nicoli, M. C. (2011). Effect of monoglyceride organogel structure on cod liver oil stability. *Food Research International, 44*, 2978-2983.

Du, A., Zhou, B., Zhang, Z. H., & Shen, J. (2013). A Special Material or a New State of Matter: A Review and Reconsideration of the Aerogel. *Materials, 6*, 941-968.

Dunstan, D. E., Chen, Y., Liao, M. L., Salvatore, R., Boger, D. V., & Prica, M. (2001). Structure and rheology of the kappa-carrageenan/locust bean gum gels. *Food Hydrocolloids, 15*, 475-484.

Escudero, R. R., Robitzer, M., Di Renzo, F., & Quignard, F. (2009). Alginate aerogels as adsorbents of polar molecules from liquid hydrocarbons: Hexanol as probe molecule. *Carbohydrate Polymers, 75*, 52-57.

Garcia-Gonzalez, C. A., Camino-Rey, M. C., Alnaief, M., Zetzl, C., & Smirnova, I. (2012). Supercritical drying of aerogels using CO2: Effect of extraction time on the end material textural properties. *Journal of Supercritical Fluids, 66*, 297-306.

Gesser, H. D., & Goswami, P. C. (1989). Aerogels and Related Porous Materials. *Chemical Reviews, 89*, 765-788.

Gordon, M., & Taylor, J. S. (1952). Ideal copolymers and the second-order transitions of synthetic rubbers. i. non-crystalline copolymers. *Journal of Applied Chemistry, 2*, 493-500.

Hrubesh, L. W., & Poco, J. F. (1995). Thin Aerogel Films for Optical, Thermal, Acoustic and Electronic Applications. *Journal of Non-Crystalline Solids, 188*, 46-53.

Ivanovic, J., Milovanovic, S., & Zizovic, I. (2016). Utilization of supercritical CO2 as a processing aid in setting functionality of starch-based materials. *Starch - Stärke, 68*, 821-833.

Khosravi, M., & Azizian, S. (2016). A new kinetic model for absorption of oil spill by porous materials. *Microporous and Mesoporous Materials, 230*, 25-29.

505 Laredo, T., Barbut, S., & Marangoni, A. G. (2011). Molecular interactions of polymer
506 oleogelation. *Soft Matter, 7*, 2734-2743.
507 Mallepally, R. R., Bernard, I., Marin, M. A., Ward, K. R., & McHugh, M. A. (2013).
508 Superabsorbent alginate aerogels. *Journal of Supercritical Fluids, 79*, 202-208.
509 Mikkonen, K. S., Parikka, K., Ghafar, A., & Tenkanen, M. (2013). Prospects of
510 polysaccharide aerogels as modern advanced food materials. *Trends in Food Science*
511 *& Technology, 34*, 124-136.
512 Nikiforidis, C. V., & Scholten, E. (2015). Polymer organogelation with chitin and chitin
513 nanocrystals. *RSC Advances, 5*, 37789-37799.
514 Patel, A. R., & Dewettinck, K. (2016). Edible oil structuring: an overview and recent updates.
515 *Food & Function, 7*, 20-29.
516 Patel, A. R., Rajarethinem, P. S., Gredowska, A., Turhan, O., Lesaffer, A., De Vos, W. H.,
517 Van de Walle, D., & Dewettinck, K. (2014). Edible applications of shellac oleogels:
518 spreads, chocolate paste and cakes. *Food & Function, 5*, 645-652.
519 Patel, A. R., Schatteman, D., Lesaffer, A., & Dewettinck, K. (2013). A foam-templated
520 approach for fabricating organogels using a water-soluble polymer. *Rsc Advances, 3*,
521 22900-22903.
522 Pierre, A. C., & Pajonk, G. M. (2002). Chemistry of aerogels and their applications. *Chemical*
523 *Reviews, 102*, 4243-4265.
524 Rinaudo, M. (2008). Main properties and current applications of some polysaccharides as
525 biomaterials. *Polymer International, 57*, 397-430.
526 Rochas, C., & Rinaudo, M. (1984). Mechanism of gel formation in k-carrageenan.
527 *Biopolymers, 23*, 735-745.
528 Scherer, G. W., & Smith, D. M. (1995). Cavitation during Drying of a Gel. *Journal of Non-*
529 *Crystalline Solids, 189*, 197-211.

530 Stortz, T. A., & Marangoni, A. G. (2013). Ethylcellulose solvent substitution method of
531 preparing heat resistant chocolate. *Food Research International, 51*, 797-803.
532 Tanti, R., Barbut, S., & Marangoni, A. G. (2016a). Hydroxypropyl methylcellulose and
533 methylcellulose structured oil as a replacement for shortening in sandwich cookie
534 creams. *Food Hydrocolloids, 61*, 329-337.
535 Tanti, R., Barbut, S., & Marangoni, A. G. (2016b). Oil stabilization of natural peanut butter
536 using food grade polymers. *Food Hydrocolloids, 61*, 399-408.
537 Therkelsen, G. H. (1993). Carrageenan. In R. L. Whistler & J. N. BeMiller (Eds.), *Industrial*
538 *Gums: Polysaccharides and Their Derivatives* (Third ed., pp. 146-176). San Diego
539 (USA): Academic Press, Inc.
540 Yilmaz, E., & Ogutcu, M. (2015). The texture, sensory properties and stability of cookies
541 prepared with wax oleogels. *Food & Function, 6*, 1194-1204.
542 Zetzl, A. K., Marangoni, A. G., & Barbut, S. (2012). Mechanical properties of ethylcellulose
543 oleogels and their potential for saturated fat reduction in frankfurters. *Food &*
544 *Function, 3*, 327-337.
545 Zulim Botega, D. C., Marangoni, A. G., Smith, A. K., & Goff, H. D. (2013). The potential
546 application of rice bran wax oleogel to replace solid fat and enhance unsaturated fat
547 content in ice cream. *Journal of Food Science, 78*, C1334-1339.

548

549 Table 1. Network density and firmness of hydrogel containing increasing κ-carrageenan
550 concentration, and of the derived alcoholgel and aerogel.

κ-carrageenan in hydrogel (% w/w)	Network density ($g_{d.m.}/cm^3$)			Firmness (N)		
	Hydrogel	Alcoholgel	Aerogel	Hydrogel	Alcoholgel	Aerogel
0.4	0.004 ± 0.001[c]	0.009 ± 0.001[b]	0.237 ± 0.026[a]	0.84 ± 0.06[c]	8.00 ± 0.66[c]	114.00 ± 7.21[a]
1	0.008 ± 0.001[b]	0.014 ± 0.002[b]	0.180 ± 0.014[ab]	3.37 ± 0.05[b]	18.92 ± 0.94[b]	165.67 ± 7.22[b]
2	0.016 ± 0.001[a]	0.026 ± 0.003[a]	0.129 ± 0.001[b]	7.37 ± 0.70[a]	45.22 ± 1.50[a]	136.67 ± 2.03[a]

551 [a, b, c]: means with different letters in the same column are significantly different ($p < 0.05$).

552

553 Table 2. Experimental regression coefficients estimates m_0 ($g_{H_2O}/g_{d.m.}$) and c for BET equation
554 ($R^2 > 0.85$; $p < 0.05$), and k for Gordon-Taylor equation ($R^2 > 0.93$; $p < 0.001$) of aerogels
555 obtained from hydrogels containing increasing κ-carrageenan concentration. Standard error of
556 fitting is also reported.

κ-carrageenan in hydrogel	BET equation			Gordon-Taylor equation	
(% w/w)	m_0 ± SE	c ± SE	R^2	k ± SE	R^2
0.4	0.04 ± 0.01	9.23 ± 6.16	0.95	10.33 ± 1.55	0.97
1.0	0.05 ± 0.01	43.88 ± 13.91	0.85	9.79 ± 1.27	0.93
2.0	0.04 ± 0.01	4.86 ± 0.52	0.99	9.92 ± 0.94	0.98

557

558

559 Table 3. Experimental regression coefficients estimates k_{fast}, k_{slow}, and y_{max} for the two-phase
560 model of oil absorption in aerogels obtained from hydrogels containing increasing κ-
561 carrageenan concentration. Standard error of fitting is also reported.

	κ-carrageenan in hydrogel (% w/w)		
	0.4	1.0	2.0
k_{fast} (h^{-1})	3.825 ± 0.320	2.080 ± 0.153	1.734 ± 0.198
k_{slow} (h^{-1})	0.602 ± 0.058	0.313 ± 0.017	0.139 ± 0.006
y_{max} ($g_{oil}/g_{aerogel}/cm^3_{aerogel}$)	1.077 ± 0.049	3.195 ± 0.112	13.845 ± 0.310

562

563

564 Table 4. Visual appearance, firmness, oil content, and oil holding capacity (OHC) of oleogels
565 obtained from hydrogels containing increasing κ-carrageenan concentration.

κ-carrageenan in hydrogel (% w/w)	Visual appearance	κ-carrageenan in oleogel (% w/w)	Oil in oleogel (% w/w)	Firmness (N)	OHC (% w/w)
0.4	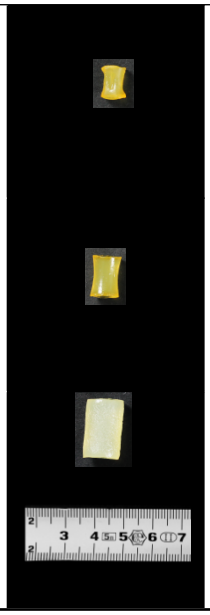	27.58 ± 0.83[a]	72.42 ± 0.83[a]	158.33 ± 9.16[c]	83.44 ± 1.35[a]
1.0		26.76 ± 0.33[a]	73.24 ± 0.33[a]	311.70 ± 11.78[a]	82.18 ± 1.11[a]
2.0		18.72 ± 0.31[b]	81.28 ± 0.31[b]	216.40 ± 6.79[b]	62.21 ± 1.31[b]

566 [a, b, c]: means with different letters in the same column are significantly different ($p<0.05$)

567

568 **Figure captions**

569 Figure 1. Schematic representation of supercritical CO_2 drying apparatus.

570

571 Figure 2. Visual appearance of hydrogel containing increasing κ-carrageenan concentration,
572 and of the derived alcoholgel and aerogel. A ruler in cm is also reported as reference. Scanning
573 electron microscopy images of aerogels obtained from hydrogels containing increasing κ-
574 carrageenan concentration.

575

576 Figure 3. Modified state diagram of aerogel obtained from hydrogel containing 1% (w/w) κ-
577 carrageenan.

578

579 Figure 4. Absorbed oil (A) and oil absorption capacity (B) of aerogels obtained from hydrogels
580 containing increasing κ-carrageenan concentration as a function of time.

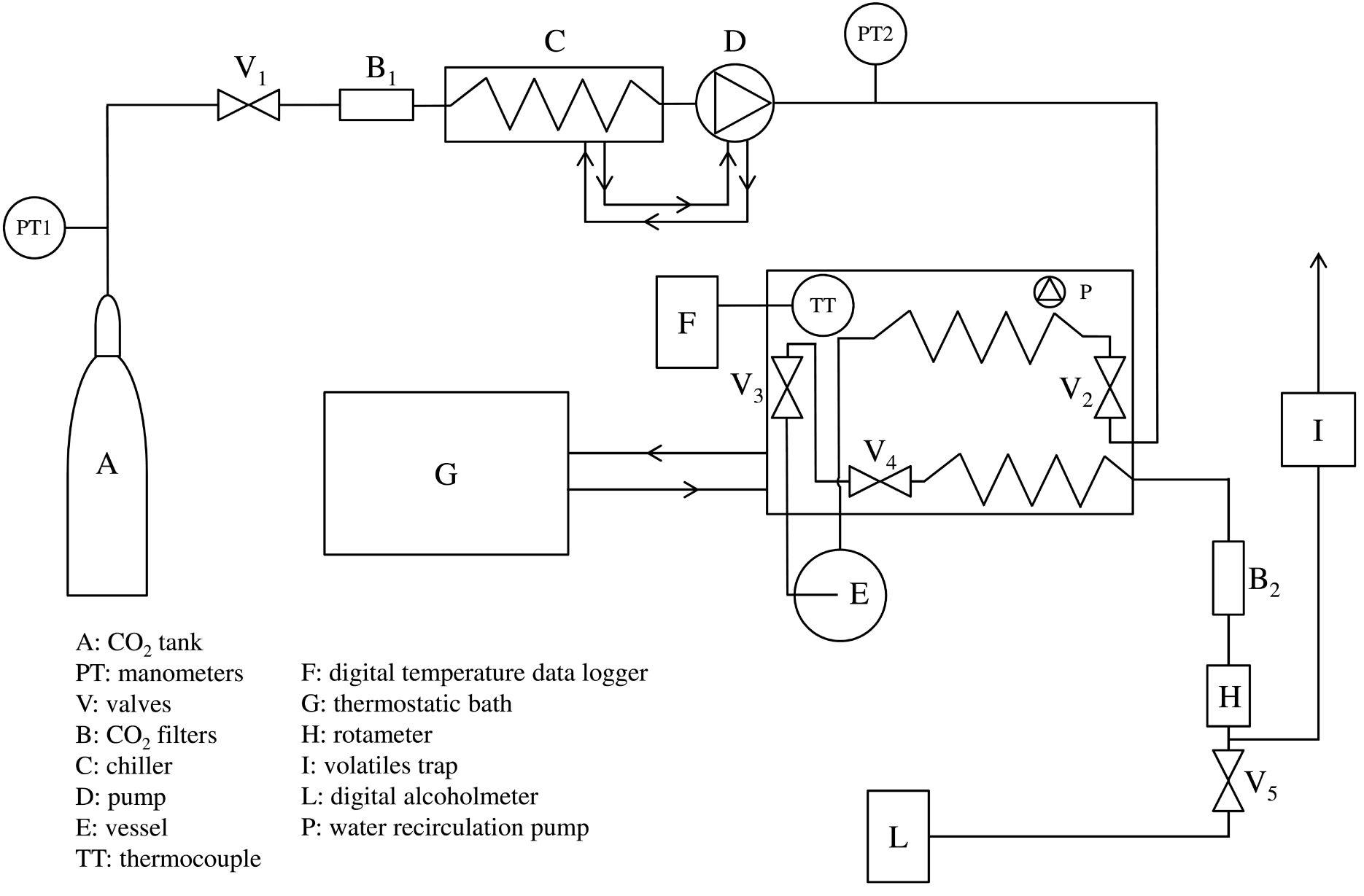

A: CO_2 tank
PT: manometers
V: valves
B: CO_2 filters
C: chiller
D: pump
E: vessel
TT: thermocouple
F: digital temperature data logger
G: thermostatic bath
H: rotameter
I: volatiles trap
L: digital alcoholmeter
P: water recirculation pump

κ-carrageenan in hydrogel (% w/w)	Hydrogel	Alcoholgel	Aerogel	Aerogel SEM images
0.4	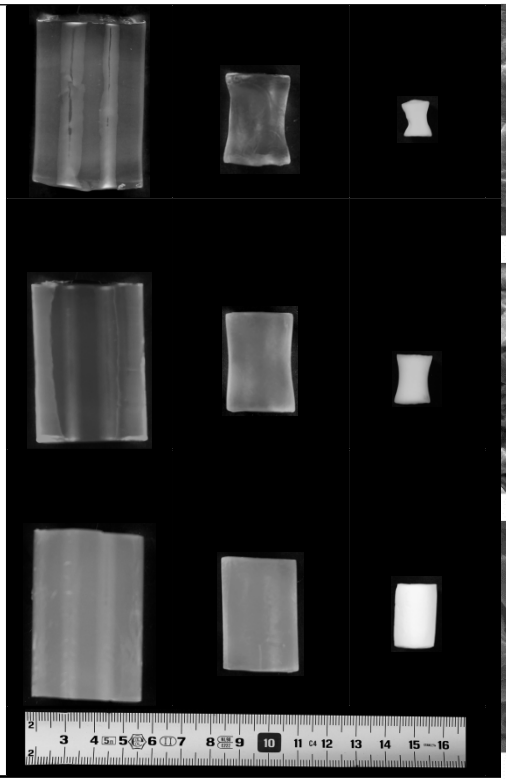			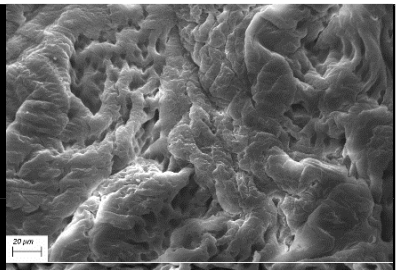
1.0				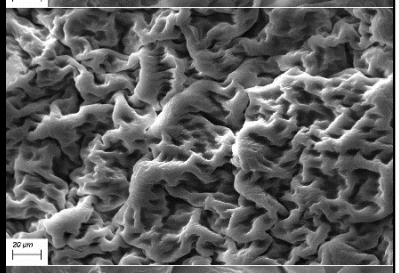
2.0				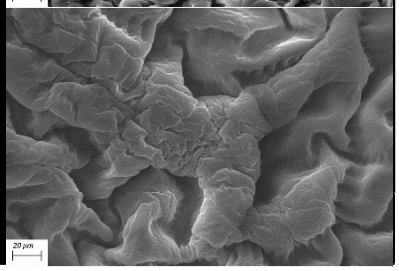

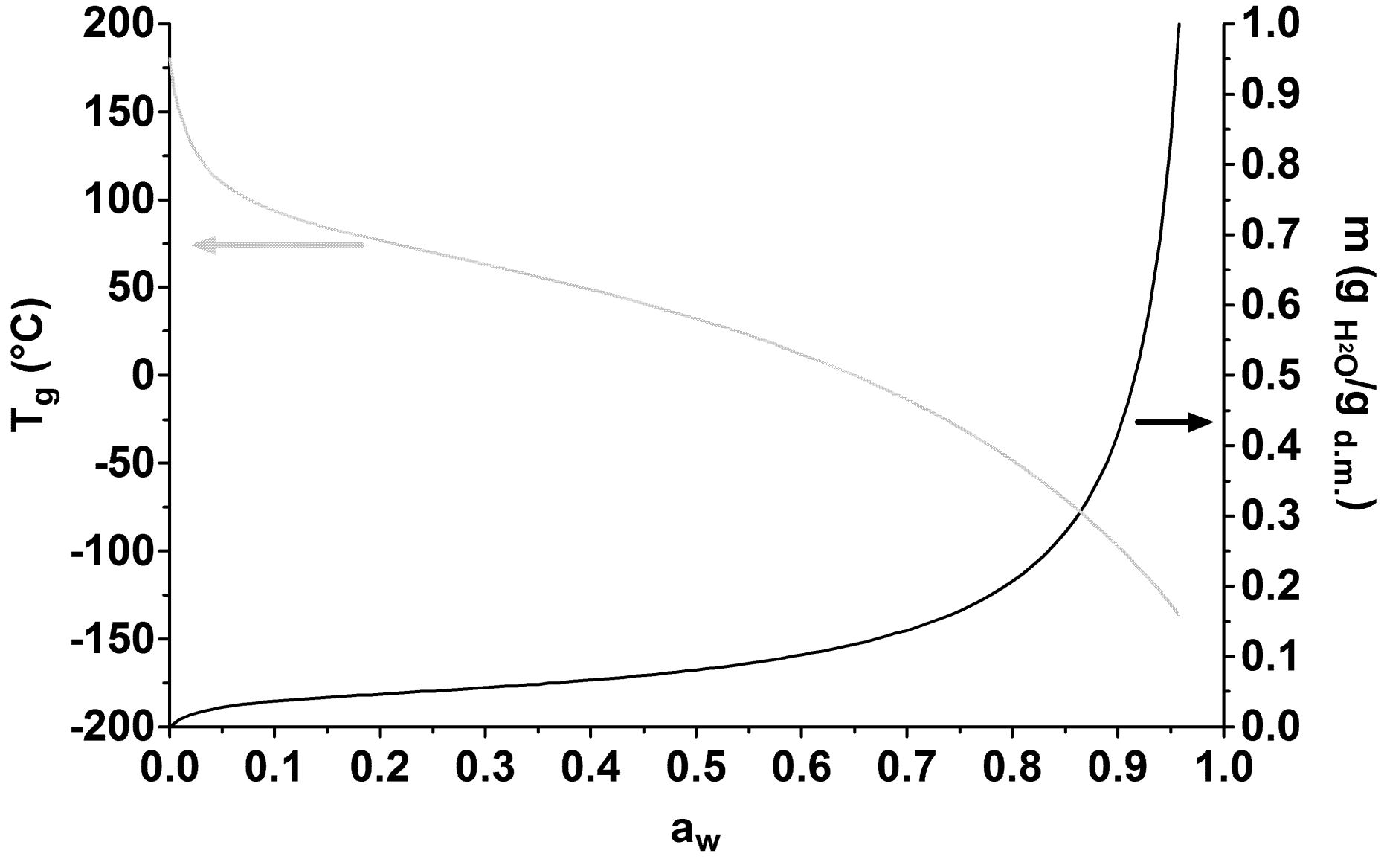
200
150
100
50
0
-50
-100
-150
-200
T_g (°C)
1.0
0.9
0.8
0.7
0.6
0.5
0.4
0.3
0.2
0.1
0.0
m (g $_{H_2O}$/g $_{d.m.}$)
0.0
0.1
0.2
0.3
0.4
0.5
0.6
0.7
0.8
0.9
1.0
a_w

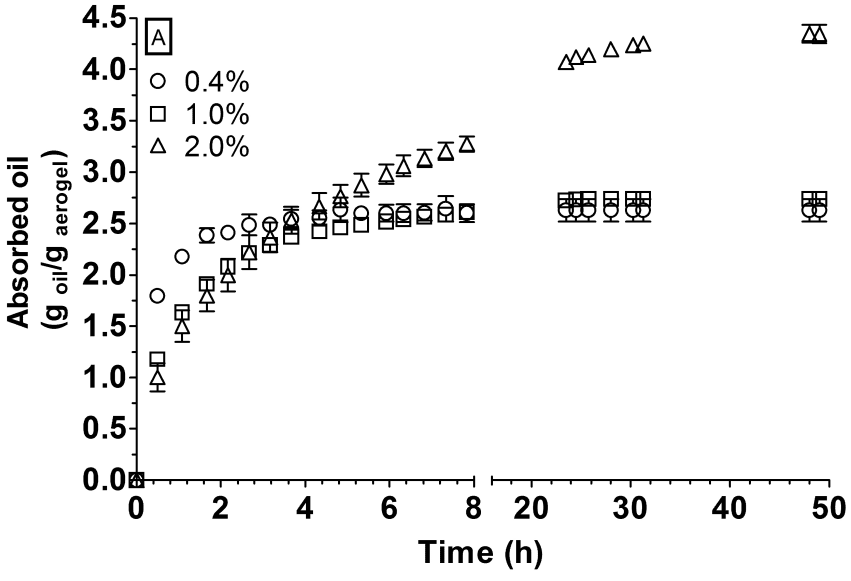
A
0.4%
1.0%
2.0%
Absorbed oil
(g oil/g aerogel)
Time (h)
0.0
0.5
1.0
1.5
2.0
2.5
3.0
3.5
4.0
4.5
0
2
4
6
8
20
30
40
50

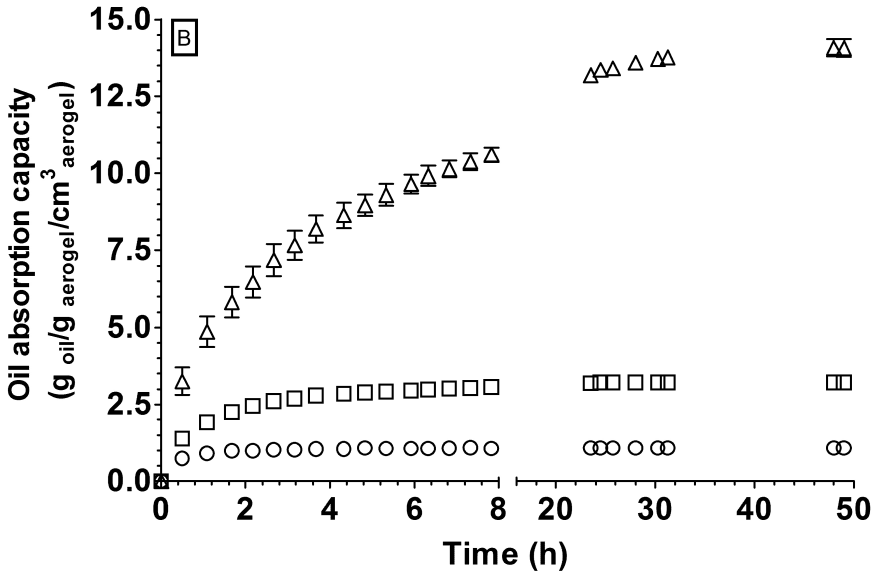
B
Oil absorption capacity
(g oil/g aerogel/cm3 aerogel)
Time (h)
0.0
2.5
5.0
7.5
10.0
12.5
15.0
0
2
4
6
8
20
30
40
50

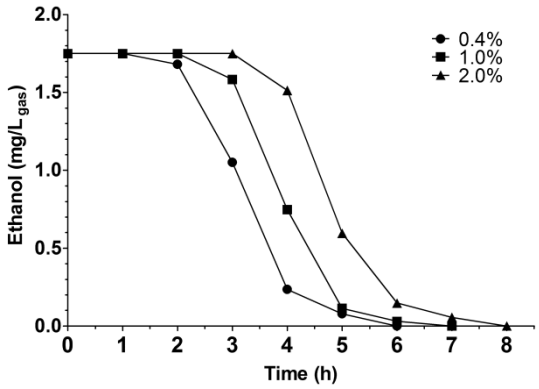

Figure S1. Ethanol concentration as a function of time during supercritical CO_2 drying of alcoholgels obtained from hydrogels containing increasing κ-carrageenan concentration.

Highlights

k-carrageenan aerogels with tailored properties can be obtained by supercritical CO_2 drying;

k-carrageenan aerogels showed high oil loaded capacity;

k-carrageenan oleogels could have interesting potential application in food area.